Science Bulletin 64 (2019) 1179–1194

Contents lists available at ScienceDirect

Science Bulletin

journal homepage: www.elsevier.com/locate/scib

Science Bulletin
www.scibull.com

Article

Inhibition of MALT1 paracaspase activity improves lesion recovery following spinal cord injury

Hua Zhang [a,1], Guodong Sun [b,1], Xiaowei Li [a], Zhen Fu [a], Chengbin Guo [a], Guangchao Cao [a], Baocheng Wang [a], Qian Wang [a], Shuxian Yang [a], Dehai Li [a], Xichun Xia [a], Peng Li [a], Jing Zhu [a], Wei Zhou [a], Liangyan Zheng [a], Jingxia Li [a], Lei Zhang [c], Jianlei Hao [a], Libing Zhou [d], Frederic Bornancin [e], Zhizhong Li [f,b,*], Zhinan Yin [a,g,*], Yunfei Gao [a,*]

[a] The First Affiliated Hospital, Biomedical Translational Research Institute and School of Pharmacy, Jinan University, Guangzhou 510632, China
[b] Department of Orthopedics, First Affiliated Hospital, Jinan University, Guangzhou 510632, China
[c] Shandong Provincial Qianfoshan Hospital, Shandong First Medical University, Jinan 250014, China
[d] Guangdong-Hongkong-Macau Institute of CNS Regeneration, Ministry of Education CNS Regeneration Collaborative Joint Laboratory, Jinan University, Guangzhou 510632, China
[e] Novartis Institutes for BioMedical Research, CH-4002 Basel, Switzerland
[f] Department of Orthopedics, Heyuan People's Hospital (Heyuan Affiliated Hospital of Jinan University), Heyuan 517199, China
[g] State Key Laboratory of Biotherapy, Collaborative Innovation Center for Biotherapy, West China Hospital, Sichuan University, Chengdu 610041, China

ARTICLE INFO

Article history:
Received 8 February 2019
Received in revised form 13 March 2019
Accepted 26 March 2019
Available online 22 April 2019

Keywords:
Anti-inflammatory macrophage
Pro-inflammatory macrophage
Spinal cord injury
NF-κB
MALT1 paracaspase activity

ABSTRACT

Spinal cord injury (SCI) is a devastating traumatic injury that causes persistent, severe motor and sensory dysfunction. Immune responses are involved in functional recovery after SCI. Mucosa-associated lymphoid tissue lymphoma translocation 1 (MALT1) has been shown to regulate the survival and differentiation of immune cells and to play a critical role in many diseases, but its function in lesion recovery after SCI remains unclear. In this paper, we generated KI (knock in) mice with a point mutation (C472G) in the active center of MALT1 and found that the KI mice exhibited improved functional recovery after SCI. Fewer macrophages were recruited to the injury site in KI mice and these macrophages differentiated into anti-inflammatory macrophages. Moreover, macrophages from KI mice exhibited reduced phosphorylation of p65, which in turn resulted in decreased SOCS3 expression and increased pSTAT6 levels. Similar results were obtained upon inhibition of MALT1 paracaspase with the small molecule inhibitor "MI-2" or the more specific inhibitor "MLT-827". In patients with SCI, peripheral blood mononuclear cells (PBMC) displayed increased MALT1 paracaspase. Human macrophages showed reduced pro-inflammatory and increased anti-inflammatory characteristics following the inhibition of MALT1 paracaspase. These findings suggest that inhibition of MALT1 paracaspase activity in the clinic may improve lesion recovery in subjects with SCI.

1. Introduction

Spinal cord injury (SCI) is a devastating traumatic injury to the spinal cord that causes persistent, severe motor and sensory dysfunction [1,2]. According to WHO studies, approximately 250,000–500,000 people worldwide suffer annually from SCI. Furthermore, people with a SCI are two to five times more likely to die prematurely. SCI is usually caused by external trauma, including accidents, falls, and sports-related injuries, rather than degenerative diseases. The effects of SCI can vary widely-from no effect, to pain, or the complete loss of spinal cord function [3,4]. Morphologically, SCI results from primary damage to the spinal cord, followed by a secondary injury. Primary damage to the spinal cord directly destroys tissues and cannot be ameliorated [5,6]. Secondary injury is believed to lead to further tissue damage, followed by permanent impairment of motor function; this damage is caused by posttraumatic inflammatory reactions and edema, and thus can be intervened [7–9]. Indeed, increased levels of pro-inflammatory cytokines, such as tumor necrosis factor (TNF) and

* Corresponding authors.
E-mail addresses: tzzli@jnu.edu.cn (Z. Li), zhinan.yin@yale.edu (Z. Yin), tyunfeigao@jnu.edu.cn (Y. Gao).
[1] These authors contributed equally to this work.

https://doi.org/10.1016/j.scib.2019.04.026
2095-9273/

IL-1β, are evident in the spinal cord within minutes of injury [10]. The subsequent overwhelming inflammatory response in the acute and subacute phases of injury, combined with the disrupted blood-spinal cord barrier, progressively exacerbates spinal cord swelling. This swelling parallels the arrival of inflammatory cells (such as macrophages, microglia, neutrophils and lymphocytes) into the spinal cord, which invade the lesion site during the first hours and days after injury [11,12]. Additionally, macrophages from the peripheral circulation and derived from resident microglia are among the main effector cells of the inflammatory response after SCI [13,14]. Macrophages/microglia contribute to secondary tissue damage in response to diseases and SCI [15]. These cells are among the first to respond to the SCI [10]. Our previous study showed that the inactivation of IFN-γ signaling in macrophages significantly reduced levels of pro-inflammatory cytokines in the cerebrospinal fluid of mice with SCI and improved functional recovery [12]. Two major subsets of macrophages have been distinguished, based on their functional phenotype: classically activated, pro-inflammatory macrophage, and alternatively activated, anti-inflammatory macrophage [16–18]. The differentiation of macrophages into the pro-inflammatory macrophages or anti-inflammatory macrophages predominantly determines whether these cells aggravate secondary injury or promote wound repair [19,20]. Pro-inflammatory macrophages are observed during the acute response to trauma and release high levels of reactive oxygen species [18,21]. Through increased phagocytosis and the release of pro-inflammatory cytokines, such as IL-1β, IL-6, and TNF, pro-inflammatory macrophages facilitate innate immunity to remove foreign microbes and wound debris from the injury site. Anti-inflammation macrophages exhibit tissue repair by producing anti-inflammatory cytokines such as IL-4, IL-10, and IL-13 [13,18,19,22,23].

Mucosa-associated lymphoid tissue lymphoma translocation 1 (MALT1) has recently emerged as a key point in convergence of various signaling pathways in both innate and adaptive immune cells to regulate immunity and inflammation [24–26]. MALT1 induces the activation of the NF-κB pathway using two distinct mechanisms. First, MALT1 functions as a scaffold protein, leading to TRAF6-dependent NF-κB activation [27]. Second, MALT1 functions as a cysteine paracaspase, which catalytically processes the cleavage of negative regulators of NF-κB, such as RelB, A20, and cylindromatosis (CYLD), fueling NF-κB activation [28–31]. Based on the finding that MALT1 paracaspase activity is required for immune cell activation and proliferation, researchers have hypothesized that MALT1 is a promising therapeutic target for autoimmunity and cancer [32]. Previous study showed that deficiency of MALT1 paracaspase activity deficient would promote recovery from central nervous system injury, such as multiple sclerosis (MS) [33] and experimental autoimmune encephalitis (EAE) [34]. Additionally, similar to MS and EAE, SCI is also characterized by an immune response that targets the central nervous system (CNS). However, it is not yet determined whether MALT1 participates in immune responses after SCI.

In this study, we reported that MALT1 paracaspase activity plays a critical role in a mouse model of SCI. We generated MALT1 KI mice expressing a catalytically inactive form of MALT1 that maintains its scaffold function to investigate the effects of MALT1 paracaspase inactivation on the immune response after SCI in vivo. A small molecule inhibitor, MI-2, which forms a covalent bond in the active site, was used to inhibit the paracaspase activity of MALT1 [35]. In addition, a potent and specific inhibitor, MLT-827, was also used to inhibit the paracaspase activity of MALT1 [36,37]. We hypothesized that deficiency or inhibition of MALT1 paracaspase activity in mice would promote functional recovery from SCI. Upon suppression of the MALT1 paracaspase activity, macrophages decreased the phosphorylation of p65, which resulted in the down-regulation of inflammatory cytokines and SOCS3 expression and increased levels of pSTAT6, and adopted an anti-inflammatory phenotype. Moreover, human macrophages showed a similar functional phenotype upon treatment with the MALT1 inhibitors. Thus, MALT1 paracaspase activity may represent a potentially novel therapeutic target for treating SCI.

2. Materials and methods

2.1. Mice

C57BL/6J mice were purchased from The Jackson Laboratory (Bar Harbor, ME, USA). MALT1 KI mice were generated from Cyagen Biosciences (Guangzhou, China), bred and maintained in the animal facility at Jinan University (Guangzhou, China). All mice were females, aged 7–8 weeks old and weighed 17–22 g at the time of surgery. All procedures were approved by and performed in accordance with the guidelines of the Institutional Laboratory Animal Care and Use Committee of Jinan University.

2.2. Generation of MALT1 KI mice

We generated MALT1 protease-deficiency C472G (a cysteine-to-glycine mutation was introduced at position 472) mice from Cyagen Biosciences (Guangzhou China). Full-length MALT1 contains: a death domain (DD) and two Ig domains at the N-terminal region, and a paracaspase domain (including the active site residues C472) and Ig fold at the C-terminal half. We amplified mouse MALT1 sequences from C57BL/6 mouse genomic DNA, and then generated genetically modified mice by homologous recombination with a targeting vector carrying a TGTGT to TGGGT mutation (nucleotides 165–169 of exon 10) encoding a catalytically inactive mutant of MALT1 protein. This mutation of MALT1 in offspring was confirmed by nucleotide sequencing and PCR with tail DNA. Nucleotide sequencing showed the nucleotide T at 168 was mutated to G. After confirming correctly targeted ES clones via Southern Blotting, we selected some clones for blastocyst microinjection, followed by chimera production.

Our C472G mice (number based on MALT1 isoform B) are, in fact, equivalent to the previously described C472A KI mice (number based on MALT1 isoform A) [38], except for replacing the cysteine by a glycine, rather than by an alanine. Both isoforms exist and are differentially regulated [39]. The C472G KI mice were back crossed with C57BL/6J for at least 5 generations. The detail location of C472G, the construct, sequence confirmation, and PCR products of KI mice were presented in Supplementary data (Fig. 1 Sa-d, online).

The C472G KI mice were normal without obvious impairments in appearance or organ defects before 6 weeks of age. However, a portion of male mice (about 30%–50%) developed spontaneous autoimmune diseases (dermatitis and skin ulcerations in neck, mouth and tail) starting from 6 weeks and worsening as age increased. However, most of the female mice remained normal (Fig. S2 online) and autoimmune symptoms were relatively rare. This was inconsistent with previous reports that stated C472A female mice also developed spontaneous autoimmune diseases [38]. This discrepancy is interesting and needs further exploration. During our research, all animal experiments were carried out using female mice at 7–8 weeks of age without any sign of autoimmune diseases.

2.3. Reagents

PE-conjugated anti-mouse F4/80 (M100F1-09B), the β-actin mAb (KM9001T) and –the mouse monoclonal tubulin antibody

(KM9003) were purchased from Tianjin Sungene (Tianjin, China). Recombinant human MCSF (30025), recombinant human IFN-γ (30002), recombinant human IL-4 (20004), recombinant mouse MCSF (31502), recombinant mouse IFN-γ (31505), and recombinant mouse IL-4 (21414) proteins were purchased from Peprotech (Rocky Hill, NJ, USA). The arginase 1 antibody (GTX109242) and iNOS antibody (GTX74171) were purchased from Gentex (Alton Parkway Irvine, CA, USA). The PE-conjugated anti-human CD14 antibody (367104) and biotin-conjugated anti-human CD14 antibody (325624) were purchased from Biolegend (San Diego, CA, USA). The phospho-IκBα (ser32) (14D4) rabbit mAb (2859), IκBα rabbit mAb (4812), phospho-p65 (ser536) rabbit mAb (3031), NF-κB (p65) rabbit mAb (8242), and STAT6 (D3H4) rabbit mAb (5397) were purchased from Cell Signaling Technology (Danvers, MA, USA). The anti-F4/80 antibody (ab16911) and anti-STAT6 (phosphor Y641) antibody (56554) were purchased from Abcam (Cambridge, MA, USA). The rabbit CYLD antibody (11110-1-AP) was purchased from Proteintech (Chicago, IL, USA). MALT1 (H-300) (sc-28246) was purchased from Santa Cruz Biotechnology (Santa Cruz, CA, USA). LPS was purchased from Sigma (St. Louis, MO, USA). The Alexa Fluor® 594-conjugated goat anti-mouse IgG (H + L) antibody (A11032) and Alexa Fluor® 488-conjugated goat anti-rabbit IgG (H + L) antibody (A28175), which were highly cross-adsorbed, were purchased from Thermo Fisher Scientific (Waltham, MA, USA). The Easy Pure RNA Kit was purchased from TRAN (Beijing, China). BSA and Triton X-100 were purchased from VETEC (St. Louis, MO, USA).

2.4. Inhibitor of MALT1

MI-2 (Selleck, Texas, USA) was dissolved at a concentration of 90 mg/mL (for in vitro, diluted with PEG300) and 30 mmol/L (for in vivo, diluted in DMSO) as a stock solution, stored at −20 °C, and diluted with medium before each experiment. The final DMSO concentration did not exceed 0.01% throughout the study (all the control groups were composed of 0.01% DMSO).

MLT-827 was dissolved in a concentration of 10 mmol/L in DMSO as a stock solution and stored at −20 °C [40]. The final DMSO concentration did not exceed 0.01% throughout the study (all the control groups received 0.01% DMSO).

2.5. Cell culture, shift and identification of BMDMs

The culture, shift and characterization of BMDMs were performed using previously described methods. BMDMs were isolated from C57/BL6 mice and MALT1 mutant mice. Specifically, BMDMs were flushed from the femur with a solution containing 1% penicillin/streptomycin and sterilized phosphate-buffered saline (PBS), pH 7.4; then, red cells were removed and BMDMs were cultured with DMEM, supplemented with 20 ng/mL MCSF (murine), 1% penicillin/streptomycin, and 10% fetal calf serum in a humidified 5% (v/v) CO_2 atmosphere at 37 °C. The culture medium was exchanged with fresh culture medium every 3 days. Under these conditions, adherent macrophages were obtained after 7 days. Cells were cultured without MCSF for 6 h, and then stimulated to differentiate into pro-inflammatory macrophages by addition of LPS (100 ng/mL) plus IFN-γ (10 ng/mL), or into anti-inflammatory macrophages using IL-4 (10 ng/mL). Twelve hours after incubation, RNA and protein were isolated from the stimulated macrophages.

2.6. Isolation of human monocytes and differentiation into hMDMs

PBMCs were isolated from blood donors (control without SCI) using ACK lysis buffer. Cells were then washed twice, and monocytes were obtained by the positive selection of $CD14^+$ cells. Cells were cultured with complete DMEM supplemented with 50 ng/mL MCSF (human), and seeded in a dilution of $1–2 \times 10^6$ cells/mL. After 3 days of culture, adherent cells were washed twice with PBS to remove MCSF. The medium was then exchanged for fresh medium. Cells were cultivated for 7–8 days at 37 °C in a 5% CO_2 atmosphere to promote their complete differentiation into hMDMs. These hMDMs were then stimulated with either LPS (100 ng/mL) plus IFN-γ (20 ng/mL) for 6 h or IL-4 (20 ng/mL) for 18 h to obtain pro-inflammatory macrophages or anti-inflammatory macrophages, respectively.

2.7. Sample collection from clinical patients

Patients sustaining an acute SCI were recruited at the First Affiliated Hospital of Jinan University and the Heyuan Affiliated Hospital of Jinan University by neurosurgeons from May 2013 to May 2016. Inclusion criteria for the trial were: ASIA grade A or B SCI upon presentation, spinal injury between C4 and T12 (inclusive), presentation within 48 h post-injury, and the ability to provide a valid, reliable neurological examination. Patients were excluded if they had concomitant head injuries, concomitant major trauma to the chest, pelvis, or extremities that required invasive intervention (e.g., chest tube, internal or external fixation), or if they were too sedated or intoxicated to provide a valid neurological examination. We enrolled individuals with hip osteoarthritis who were undergoing hip replacements under spinal anesthesia to obtain control samples from patients without an SCI. The clinical trial protocol was approved by the Human Ethics Committee at Jinan University, and the sample collection was approved by individual patients. Patient, Control group (volunteer), and Control group (hip osteoarthritis) demographics and baseline neurological status were as stated in Tables 1–3.

2.8. Immunofluorescence staining

BMDMs and MDMs growing on coverslips were fixed with 4% paraformaldehyde, permeabilized with 1% Triton X-100 for 1 h at 37 °C and then blocked with 5% BSA for 1 h. Cells were immunostained with monoclonal anti-mouse F4/80 and anti-iNOS or anti-Arg1 Ab overnight. Then, Alexa Fluor 488-conjugated anti-rabbit IgG and Alexa Fluor 594-conjugated anti-rabbit IgG were incubated with cells for 1 h. The cells on the coverslips were counterstained with DAPI and imaged with a confocal laser scanning microscope.

2.9. Western blotting

Cells were collected and lysed in lysis buffer for 30 min. After centrifugation at 12,000 *g* for 20 min, the protein content of the supernatant was determined using a BCA™ protein assay kit. Immunoblotting was performed using previously described methods [41]. Proteins were separated on 12% Bis-Tris SDS-PAGE gradient gels and transferred to polyvinylidence difuoride membranes, and then incubated with the indicated antibodies. Finally, proteins were detected by Bio-rad ChmiDoc MP.

2.10. FACS analysis

FACS stainings of cell suspensions were prepared by passing tissues through a 40 μm sieve followed by RBC lysis using ACK buffer. Cells were washed once in FACS buffer (PBS containing 2% BSA), and stained for 20 min at 4 °C with indicated combination of fluorochrome-conjugated Abs. After staining, the cells were washed twice and resuspended in 200 μL buffer before acquisition on BD FACSAria. Data were analyzed using the FlowJo software.

Table 1
Patient demographics and baseline neurological status.

ID	Mechanism of injury	Spinal injury	Age	Sex	ASIA grade	Level
1	MVA	T7/T8 fracture-dislocation	37	M	A	Thoracic
2	Fall from standing height	T1 burst fracture	25	M	B	Thoracic
3	MVA	C6/7 fracture-dislocation	36	M	B	Cervical
4	MVA	C5/6 fracture-dislocation	36	M	A	Cervical
5	MVA	T12 burst fracture	33	M	A	Thoracic
6	MVA	T9/T10 fracture dislocation	45	M	A	Thoracic
7	Fall from standing height	T4 burst fracture	21	M	A	Thoracic
8	Diving	C6/7 fracture-dislocation	36	M	B	Cervical
9	MVA	C4/5 fracture-dislocation	28	F	A	Cervical
10	Fall from standing height	C5/6 flexion-distraction	39	M	B	Cervical
11	Fall from standing height	T9 & T10 burst fractures	41	F	B	Thoracic
12	MVA	T10 burst fracture	32	M	A	Thoracic
13	MVA	T1 burst fracture	25	M	A	Thoracic
14	MVA	T6 burst fracture	33	M	A	Thoracic
15	MVA	T12 burst fracture	50	M	A	Thoracic
16	Fall from standing height	T8 burst fracture	46	M	B	Thoracic
17	MVA	C6/7 fracture-dislocation	33	M	A	Cervical
18	MVA	T11/T11 fracture dislocation	26	F	A	Thoracic
19	MVA	T6 &T7 burst fractures	36	M	A	Thoracic
20	MVA	T8 & T9 burst fractures	42	M	A	Thoracic
21	Fall from standing height	T8 & T9 burst fractures	31	M	A	Thoracic
22	Fall from standing height	C5/6 flexion-distraction	30	F	B	Cervical
23	Fall from standing height	C3/4 flexion-distraction	37	M	A	Cervical
24	MVA	C5/6 flexion-distraction	36	M	A	Cervical
25	MVA	T1 burst fracture	35	M	B	Thoracic
26	MVA	T10 burst fracture	22	F	A	Thoracic
27	MVA	T7 burst fracture	28	M	A	Thoracic
Total			34.18 ± 7.03 years	22 male 5 female	19A,8B	9 cervical 18 thoracic

MVA: motor vehicle accident.

Table 2
Control group (volunteer).

ID	Age	Sex	ASIA grade
1	26	F	E
2	29	M	E
3	32	F	E
4	26	M	E
5	23	M	E
6	35	M	E
7	31	M	E
8	36	F	E
9	28	F	E
10	39	M	E
Total	34.18 ± 7.03 years	6 male 4 female	10 E

ASIA grade E: Represent normal nervous system.

Table 3
Control group (hip osteoarthritis) to detect inflammatory factors in cerebrospinal fluid (CSF).

ID	Age	Sex	ASIA grade	Level
1	66	F	E	N/A
2	75	M	E	N/A
3	86	F	E	N/A
4	56	M	E	N/A
5	73	M	E	N/A
6	45	M	E	N/A
7	71	M	E	N/A
8	76	F	E	N/A
9	58	F	E	N/A
10	69	M	E	N/A
Total	75 ± 11.77 years	6 male 4 female	10 E	N/A

ASIA grade E: Represent normal nervous system.

2.11. Quantitative real-time reverse transcription-PCR (RT-PCR)

The Easy Pure RNA Kit was used to isolate RNA from BMDMs and MDMs, and total RNA concentrations were obtained using a Nanodrop 2000 spectrophotometer. Complementary DNAs were synthesized from 500 ng of total RNA using the TaKaRa reverse transcription kit. The expression levels of the target genes were measured in a mixture consisting of 1 μL of the reversed-transcribed cDNAs, 6 μL of RNase-free water, 10 μL of 2 × SensiMix SYBR and fluorescein, and 1.5 μL of primers (10 μmol/L). The quantitative RT-PCR analysis was performed using the MyIQ detection system. All primer sequences used were as shown in Table 4.

2.12. Adoptive transfer of macrophages

BMDMs were flushed from the femur with a solution containing 1% penicillin/streptomycin and sterilized phosphate-buffered saline (PBS), pH 7.4; then, red cells were removed and BMDMs were cultured with DMEM supplemented with 20 ng/mL MCSF (murine), 1% penicillin/streptomycin and 10% fetal calf serum in a humidified 5% (v/v) CO^2 atmosphere at 37 °C. The culture medium was exchanged with fresh culture medium every 3 days. Under these conditions, adherent macrophages were obtained after 7 days. Macrophages were labeled with carboxyfluorescein

Table 4
Primer sequences.

Gene	Forward primer (5′–3′)	Reverse primer (5′–3′)
iNOS	CGCTTGGGTCTTGTTCACT	TCTTTCAGGTCACTTTGGTA
CD86	ATCAAGGACATGGGCTCGTA	GAAGTTGGCGATCACTGACA
Arginase1	GCTTGCTTCGGAACTCAAC	CGCATTCACAGTCACTTAGG
CD206	CAAAAACTGACTGGGCTTCC	GCCCTTGATTCCAAAGAGTG
CCR2	GAGGTCTCGGTTGGGTTGTA	CACTGTCTTTGAGGCTTGTT
CXCL10	TCTCCATCACTCCCCTTTAC	TTCGGCAGTTACTTTTGTCT
IL-6	CCAATGCTCTCCTAACAGAT	TGTCCACAAACTGATATGCT
TNF	GTACAAGGAGAACCAAGCAA	CCGTCTTTCATTACACAGGA
IL-1β	TTCAGGCAGGCAGTATCA	GTCACACACCAGCAGGTTAT
IL-10	ACATACTGCTAACCGACTCC	CCACTGCCTTGCTCTTATT
IL-4	GAAAACTCCATGCTTGAAGAA	TCTTTCAGTGATGTGGACTTG
GAPDH	ACCCAGAAGACTGTGGATGG	ACACATTGGGGGTAGGAACA

diacetate-succinimidyl ester (CFSE). Fresh macrophages were resuspended in PBS at a density of 1×10^7 cells/mL, incubated with 5 μmol/L CFSE for 10 min at 37 °C, and then washed with ice-cold PBS 3 times. For the adoptive transfer, labeled cells were suspended in PBS at a density of 2×10^7 cells/mL, and each mouse was intravenously injected with 2×10^6 cells. Transplantation of the transferred cells in blood was detected using flow cytometry, and then the SCI was induced.

2.13. Induction of SCI and treatments

Mice (WT and mutant mice) were anesthetized with pentobarbital (50 mg/kg i.p.). A clinically relevant, moderate spinal cord contusion injury was performed at the T10/11 level using a New York University Impactor, as previously described [42]. After the transverse processes of T11 and T12 were clamped to stabilize the spine, the exposed dorsal surface of the cord was subjected to a weight drop injury using a 10 g rod dropped at a height of 6.25 mm. After the injury, the muscles and skin were closed in layers, and mice were placed in a temperature and humidity-controlled chamber. Manual bladder emptying was performed three times daily until reflex bladder emptying was established [12]. The spinal cord was exposed at the low thoracic to high lumbar area; the overlying muscle and skin were sutured, and mice were housed for 6 weeks post-injury. One group of WT mice and mutant mice was administered PBS (i.p.), and another group of WT mice was administered MI-2 (15 mg/kg, i.p.) from days 1 to 14.

2.14. Bone marrow chimeras

Bone marrow chimeras were prepared according to a previously described protocol [43]. Briefly, recipients were irradiated twice with 450 rads at a 2-h interval (a total of 900 rads). Donor bone marrow cells were intravenously injected into recipients (10^6 cells/mouse). Antibiotics were added to the drinking water for the first 4 weeks after reconstitution. At 8 weeks after reconstitution, the mice were used for the SCI model.

2.15. BMS

The BMS primary scoring system is based on a scale that ranges from 0 (complete paralysis) to 9 points (completely normal). Mice were placed on a flat surface and observed for 5 min. Hind limb motor function was scored using a single-blind method with two independent blinded observers. The mean score recorded by both observers for both hind limbs was used as the BMS of the sample.

2.16. CatWalk

The gait of mice in each group was analyzed using the CatWalk XT automated quantitative gait analysis system. Deficits in descending motor control were examined by assessing the animal's ability to navigate across a 50-cm-long runway with irregularly assigned gaps between round metal bars. In baseline training and postoperative testing sessions, every mouse was required to cross the runway (The walk floor consists of a piece of glass, at least 6 mm thick) at least three times. The entire experiment was conducted in a dark, quiet environment. The CatWalk system automatically identified and tagged each paw print and then generated a series of parameters, including paw statistics (paw print length, width, maximum contact area, mean intensity, stride length, swing, and swing speed), general parameters (average speed and cadence), step sequence parameters and base of support [44]. The Regularity Index was calculated as the number of normal step sequence patterns multiplied by four and divided by the total amount of paw placements. The MaxCotact area was estimated by determining the maximal area between limbs' contact and the walking floor. These two important parameters were employed to reflect functional recovery of injured limbs; larger values indicated better functional recovery. Catwalk was utilized as a quantitative gait analysis method. It can analyze the hind limb motor function of mice or rats (including less than 3 on the BMS scale or less than 9 on BBB scale) [45–48]. Mouse BMS score of 3 or less could detect the maximum contact area of hind limbs and gait regularity index in catwalk using the version of XT 9.0.

2.17. Nissl staining of spinal cord tissue following SCI

First, 20-μm-thick coronal sections (3 mm rostral to the epicenter) were placed in mixing solution (alcohol/chloroform, 1:1) overnight at room temperature. The following day, sections were consecutively placed in 100% alcohol, 95% alcohol, 70% alcohol, and distilled water. Subsequently, the sections were stained in 0.05% cresyl violet (pH 3.0, Sigma-Aldrich, St. Louis, MO, USA) for 10 min at 40 °C after which sections were differentiated in 95% alcohol, dehydrated in 100% alcohol, and cleared in xylene. The large and Nissl-stained anterior horn cells in the spinal cord tissue were recognized as motor neurons. Five Nissl-stained sections in every experimental mouse were randomly selected for evaluating the average number of surviving neurons in the spinal cord anterior horn.

2.18. Statistical analysis

Significance was evaluated using a two-tailed *t*-test when comparing two parameters in the data presented in the figures. For comparing data in multiple groups, one-way ANOVA was used. All data were presented as the means ± standard errors of the means. Behavioral data were analyzed using repeated measures one-way ANOVA. All statistical analyses were performed using GraphPad Prism software for Windows, version 7.01

3. Results

3.1. A Deficiency in MALT1 paracaspase activity attenuates experimental SCI

Deficiency in MALT1 paracaspase activity using a KI mice approach as well as a MALT1 paracaspase activity inhibition approach protected the CNS in a mouse EAE model by alleviating inflammatory reactions [34]. To define the role of MALT1 paracaspase activity in SCI, we generated MALT1 KI mice (using the same approach as described previously [34]). Indeed, our KI mice showed reduced cleavage of the substrate of MALT1 (CYLD, RelB and BCL10, Fig S1e online). We also confirmed the activity of two MALT1 inhibitors, namely MI-2 and MLT-827. Both inhibitors significantly reduced the cleavage of MALT1 substrates in WT cells, further confirming the activity of these two small molecules (Fig S1e). The MALT1 KI mice were normal without obvious impairments in appearance or organ defects before 6 weeks of age. However, a portion of male mice (about 30%–50%) developed spontaneous autoimmune diseases (dermatitis and skin ulcerations in neck, mouth and tail) starting from 6 weeks and worsening as age increased. However, most of the female mice remained normal (Fig. S2 online), rarely developing autoimmune symptoms. Thus, all animal experiments were carried out using female mice.

We then induced SCI in MALT1 KI mice and in MI-2 treated mice (treated with MI-2 after SCI, 15 mg/kg, i.p.) by introducing a moderate contusion at the T11 segment of the spinal cord to study the effects of a deficiency in MALT1 paracaspase activity on the recovery of motor function after SCI. We collected spinal cord tissues

from injury sites and found that the expression levels of MALT1 were largely unchanged in response to SCI (levels were not modified by the MALT1 mutation). However, the canonical substrates of MALT1, such as CYLD, A20, RelB, and Bcl10 were actively cleaved 3 days post injury, indicating an increased paracaspase activity of MALT1 in response to SCI. As expected, the activity of MALT1 was significantly reduced in MALT1 KI mice or MI-2 treated mice, as indicated by less cleavage of CYLD and BCL10 (Fig. S3 online). After SCI, mice were monitored for spontaneous hind limb movement using the Basso Mouse Score (BMS) [42]. Loco-motor function was abolished immediately after the contusion-induced SCI and was then assessed for 6 weeks following the injury. MALT1 KI mice and MI-2 treated mice recovered gradually; the BMS increased from 5 days post-injury (dpi), and peaked at 5 weeks post-injury (with an average of 4.250 ± 0.309 or 3.917 ± 0.3516, $n = 6$; Fig. 1a). In contrast, functional recovery in WT mice occurred at a significantly slower rate, with a small increase in the BMS of approximately 2.75 at 5 weeks post-injury (Fig. 1a). Significant improvements were also observed in the regularity index (76.87 ± 4.083 *vs* 47.73 ± 6.489 and 82.08 ± 6.145 *vs* 47.73 ± 6.489; Fig. 1b) and hind max contact area (0.1268 ± 0.0139 *vs* 0.08027 ± 0.01433 and 0.1359 ± 0.01727 *vs* 0.0803 ± 0.0143; Fig. 1c) in the MALT1 KI mice and MI-2-treated mice at 6 weeks post-injury compared to those in the control animals. We measured the size of the spinal cord lesions in serial horizontal sections at 6 weeks post-injury using anti-glial fibrillary acidic protein (GFAP) immunostaining to assess spinal cord structures. The lesion volume was significantly smaller in MALT1 KI mice and MI-2 treated mice than in WT mice (Fig. 1d). The improved functional recovery suggested that more neurons may have survived in MALT1 KI mice and MI-2 treated mice. We counted the number of surviving motor neurons at five different sites by performing Nissl staining: the injury site as well as its rostral and caudal sites at 1.5 and 2.5 mm. No surviving motor neurons were observed at the injury sites in all 3 groups, but more motor neurons survived at the other four sites in MALT1 KI mice and MI-2 treated mice than in the WT mice (Fig. 1e). Collectively, these results clearly indicated a detrimental effect of MALT1 paracaspase activity in SCI of mouse models.

3.2. MALT1 signaling in hematopoietic cells mediates the detrimental effects on recovery following SCI

To determine cell types responsible for MALT1 paracaspase activity in the functional recovery of SCI, we generated bone marrow chimeras (WT → WT, KI → WT, WT → KI and KI → KI). The efficiency of reconstitution in chimeras was confirmed with flow cytometry (8 weeks after reconstitution) (Fig. S4a online). We then used these chimeras for SCI model and recorded the functional recovery as described above and there were no influences on body weights, RBC, and WBC of chimeras 1 week post injury Fig. S4b, c online). Interestingly, only those chimeras using KI donor mice (KI → WT and KI → KI chimeric mice) displayed significant improvement in functional recovery, as indicated with BMS and maximum contact areas, as compared to those ones receiving cells from WT donors (WT → WT or WT → KI mice (Fig. 2a–c). Based on these results, we concluded that hematopoietic cells with MALT1 paracaspase activity were critical for the impaired neurological recovery after SCI.

3.3. MALT1 paracaspase activity in macrophages contributes to functional recovery after SCI

Based on others and our own recent findings [12], we hypothesized that macrophages in the hematopoietic compartment may be responsible for the phenotype observed in KI mice. KI mice were reconstituted with bone marrow derived macrophages (BMDM) either from WT or KI (2×10^6 cells/mouse) to test this hypothesis. The transferred macrophages were detectable in the blood of recipient mice 7 days after reconstitution (Fig. S5a online). SCI was induced in these reconstituted mice and a substantial amount of macrophages infiltrated the injury site in recipient mice 3 days post-injury (Fig. S5b online). Mice that received KI macrophages exhibited improved recovery compared with mice that received WT macrophages, as shown by higher BMS (Fig. 3a), regularity index (Fig. 3b), and greater maximum contact areas of the hind limbs (Fig. 3c). Thus, MALT1 paracaspase activity in macrophages contributed to the impaired functional recovery after SCI.

3.4. MALT1 paracaspase activity regulates macrophage shift and migration

To determine whether the MALT1 paracaspase activity in macrophages affected their differentiation, we isolated spinal cord tissue from injury site and stained F4/80, iNOS, or Arg1 for immunofluorescence analysis. The total number of macrophages (F4/80 + cells) residing in the injury site was significantly decreased in KI and MI-2 treated mice compared with WT controls (Fig. 4a). In addition, the percentage of pro-inflammatory macrophages (F4/80 + iNOS +) was also decreased, while anti-inflammatory macrophage percentage had increased significantly (Fig. 4a, b). The infiltrated macrophages were also collected from injury site 3 days post injury for FACS analysis. Consistently, the proportion and mean fluorescence intensity (MFI) of CD11c+ (pro-inflammatory macrophage) had decreased significantly in KI mice compared to those in WT mice, while those of CD206+ (anti-inflammatory macrophage) had increased significantly in KI mice compared to WT mice (Fig. 4c, d). In addition, the pro-inflammatory cytokines at the injury site had also decreased while anti-inflammatory cytokines had increased (Fig. 4e, f). These results suggested that MALT1 paracaspase activity regulates the migration and differentiation of macrophages.

To determine the role of MALT1 paracaspase activity on the migration of macrophages, BMDMs from WT mice were treated with MI-2 or PBS, labeled with CFSE and then transferred into WT recipients, and a SCI model was constructed as indicated. Three days post-injury, infiltrated cells from the injury site were collected for flow cytometry analysis, and a lesser number of labeled MI-2 treated macrophages were detected at injury site, compared to those reconstituted with untreated WT BMDMs (Fig. S6 online). Moreover, the expression of CCR2 and CXCL10, which were involved in macrophage recruitment [49–52], were significantly decreased in MALT1 KI BMDMs or MI-2 treated WT BMDMs. These results indicated that MALT1 paracaspase activity was required for the infiltration of macrophages into the injury site after SCI.

We next addressed the effects of MALT1 paracaspase activity on the shift of macrophages. BMDMs were generated from MALT1 KI or WT mice and pre-incubated with MI-2 before LPS, plus IFN-γ (pro-inflammatory macrophage) or IL-4 (anti-inflammatory macrophage) stimulation. The shift of macrophages was detected by immunofluorescence staining or realtime PCR. Consistent with the findings in vivo, deficiency in or inhibition of MALT1 protease activity reduced the shift of pro-inflammatory macrophages, but promoted the shift of anti-inflammatory macrophages *in vitro* (Fig. 4g–j).

These data revealed that MALT1 paracaspase activity played an important role in macrophage infiltration after SCI, probably via CCR2 and CXCL10, and a deficiency in MALT1 paracaspase activity biased macrophages to differentiate toward the anti-inflammatory macrophages, at the expense of the pro-inflammatory macrophages.

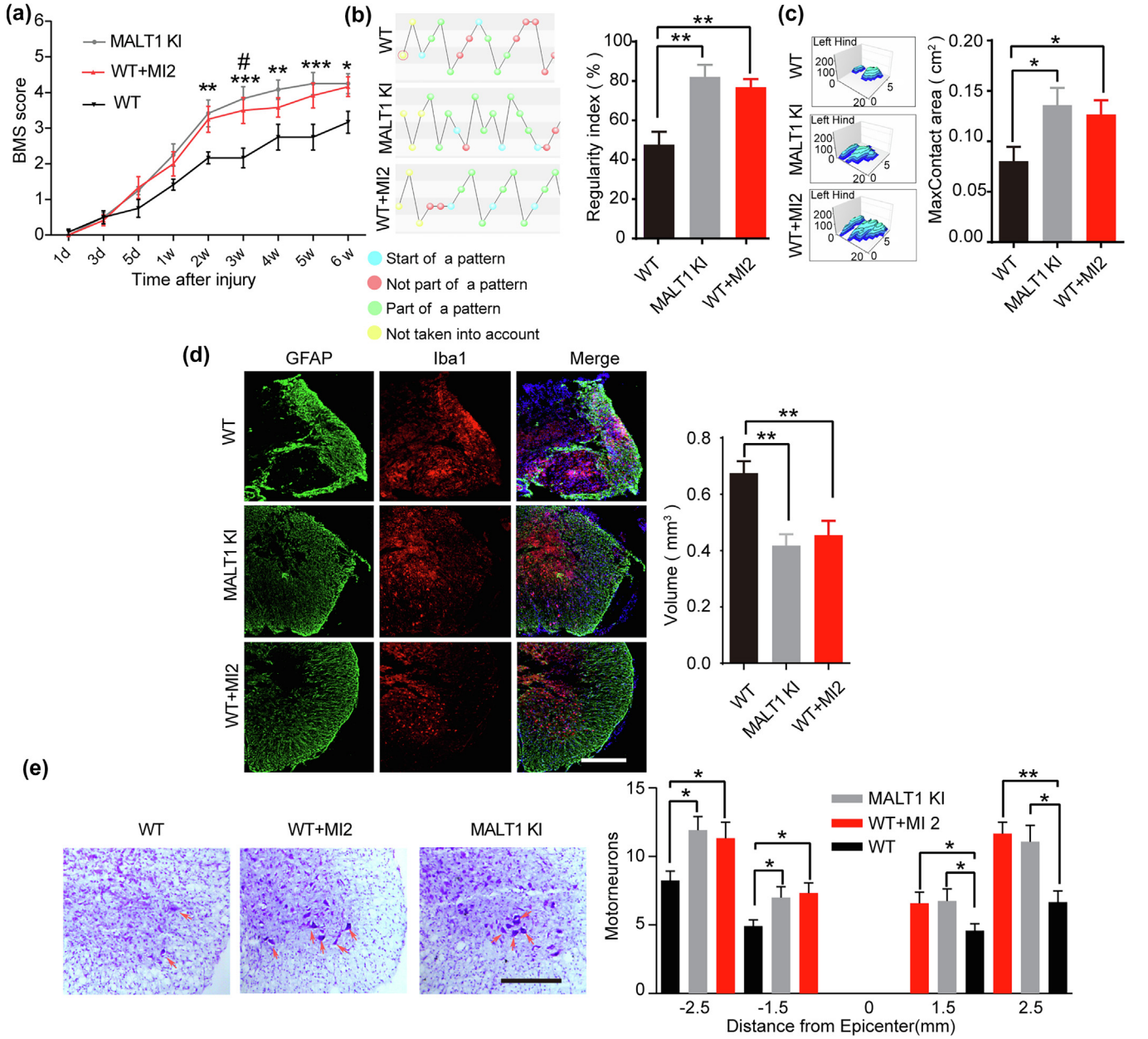

Fig. 1. Inhibition of MALT1 paracaspase activity promotes locomotor recovery in mice after SCI. (a) Mice at 8 weeks of age underwent SCI surgery and were injected i.p. with MI-2 (15 mg/kg) or PBS everyday from Day1 to Day 14. BMS (Basso Mouse Scale) of WT, MALT1 KI, and MI2-treated mice at different time points after SCI is shown ($n = 6$ mice per group). (b) Gait analysis was performed 6 weeks after SCI using the CatWalk XT system (left). Regularity index was calculated and analyzed (right, $n = 6$ mice per group). (c) The maximum hind limb contact area was analyzed 6 weeks after SCI using the CatWalk XT system, a representative diagram (left) and quantitative analysis (right) are shown ($n = 6$ mice per group). (d) The spinal cord injury sites were isolated 6 weeks post-surgery and labeled with anti-GFAP (astrocytes) and anti-Iba1 (microglia) antibodies. Representative slides are shown (left, scar bar, 250 μm). The lesion volumes were also quantitatively analyzed using the Neurolucida system ($n = 8$ mice per group). (e) The motor neurons in the spinal cord ventral horn (VH) were analyzed 6 weeks after SCI by Nissl staining (left, scale bar: 250 μm). The VH neurons at various distances from the injury epicenter were quantified (right, $n = 6$ mice per group). $^{*}P < 0.05$; $^{**}P < 0.01$; $^{***}P < 0.001$.

3.5. MALT1 paracaspase activity regulates macrophage shift through NF-κB and SOCS signaling pathways

The MALT1 paracaspase has been shown to activate NF-κB signaling in T-cells [53], and NF-κB is a critical mediator of the macrophage-dependent inflammatory response [54,55]. To determine the underlying molecular mechanisms of MALT1-mediated macrophage shift, BMDMs from WT, MALT1 KI, and MALT1 KO mice were pretreated with MI-2, MLT-827, or PBS and then stimulated with LPS, and levels of NF-κB signaling, including p-p65, IκBα and p-IκBα were analyzed through confocal microscopy and Western blot. Confocal microscopy analysis showed that p65 efficiently translocated from the cytosol into the nucleus in WT BMDMs in response to LPS, but MALT1 mutation or pharmacological inhibition of MALT1 blocked this process (Fig. 5a). In addition, the phosphorylation of p65 was reduced, along with decreased cleavage of CYLD and RelB in MALT1 KI or MI-2/MLT-827 treated cells. These results clearly indicated a halted paracaspase activity of MALT1 and reduced NF-κB signaling in these cells. However, the phosphorylation and degradation of IκB, as well as the expression of MALT1-protein, were largely unchanged in MALT1 KI or MI-2/MLT-827 treated macrophages compared with untreated WT cells,

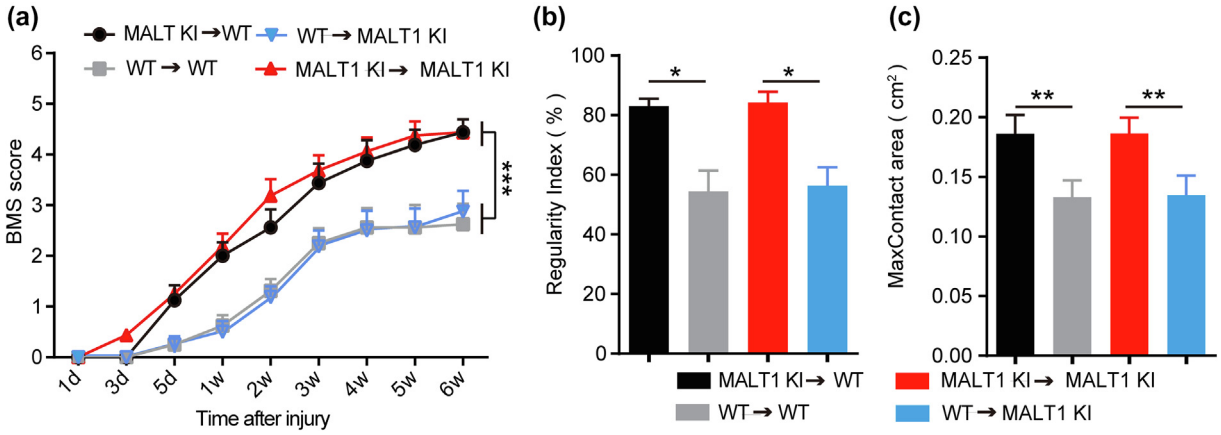

Fig. 2. MALT1 paracaspase activity in hematopoietic cells impairs recovery after SCI. Irradiated WT or MALT1 KI mice were reconstituted with bone marrow cells (1×10^6 cells/mouse) from WT or MALT1 KI mice and housed for 8 weeks for the regeneration of hematopoietic system. Chimera mice were then used for SCI surgery. (a) BMS score of chimera mice at different time points after SCI ($n = 8$ mice per group) (b,c) The regularity index and the maximum hind limb contact area were measured 6 weeks post SCI ($n = 8$ mice per group). $^{*}P < 0.05$, $^{**}P < 0.01$, $^{***}P < 0.001$.

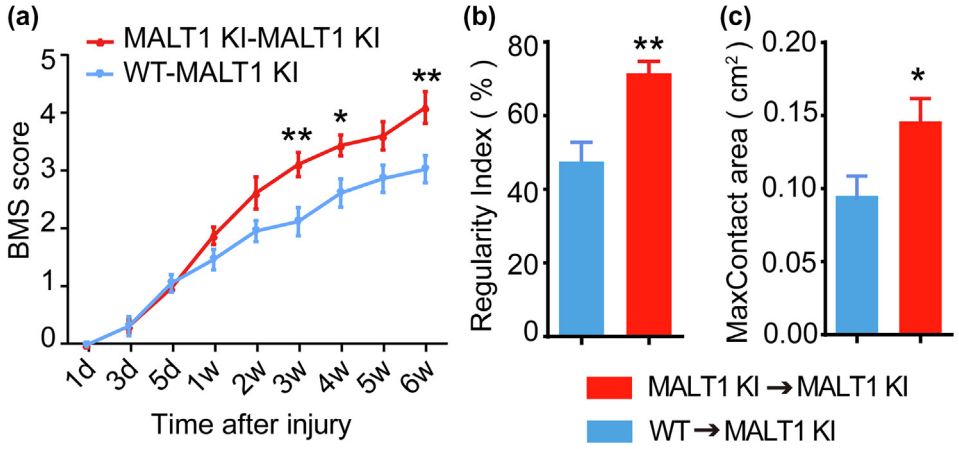

Fig. 3. Macrophage MALT1 paracaspase activity contributes to impaired neurological recovery after SCI. Bone marrow derived macrophages from WT or MALT1 KI mice were transferred into MALT1 KI mice (2×10^6 cells/mouse) and then used for SCI surgery. (a) BMS score at different time points after SCI, w: weeks. (b,c) The regularity index and maximum hind limb contact area of mice were evaluated 6 weeks post SCI ($n = 8$ mice per group). $^{*}P < 0.05$, $^{**}P < 0.01$, $^{***}P < 0.001$.

in contrast with MALT1 KO BMDMs (Fig. 5b). This is consistent with previous characterization of MALT1 protease deficiency, as compared to MALT1 protein deficiency [34,38,56].

NF-κB signaling has been reported to up-regulate the expression of SOCS family members, which inhibit the phosphorylation of STAT6, ultimately biasing macrophages to differentiate into pro-inflammatory macrophages [57,58]. Therefore, we next investigated the regulatory effects of MALT1 paracaspase activity on the expression of SOCS and STAT family members. We cultured WT, MALT1 KI, MALT1 KO and MI-2-treated or MLT-827-treated BMDMs under pro-inflammatory and anti-inflammatory conditions, and then detected the expression of SOCS proteins by Western blotting. Levels of iNOS and SOCS3 were significantly reduced in BMDMs from either KI or MALT1 inhibitor treated (both MI-2-treated and MLT-827-treated ones) cultured under pro-inflammatory conditions (Fig. 5c); meanwhile, in the same experiment, but under anti-inflammatory conditions, levels of Arg1, p-STAT6 had increased dramatically in BMDMs when MALT1 proteolytic function was compromised (Fig. 5d). Collectively, MALT1 paracaspase deficiency attenuated NF-κB signaling, down-regulated SOCS3 expression and increased phosphorylation of STAT6, ultimately causing macrophages to adopt the anti-inflammatory response.

3.6. The paracaspase MALT1 is involved in human SCI

To investigate whether pro-inflammatory cytokines are present in the injured spinal cord of patients with SCI, cerebrospinal fluid (CSF) samples were collected from 27 patients with thoracic or cervical segment injuries (Table 1) and from patients with hip osteoarthritis (which was trauma control) (Table 2). Levels of pro-inflammatory cytokines IL-6, TNF-α, IFN-γ, MCP-1 and MIP-1α were significantly increased in the CSF of patients compared to trauma controls, while the levels of anti-inflammatory cytokines IL-4 were not affected (Fig. S8 online), which is consistent with our previous publication (12), Furthermore, the ratio of pro-inflammatory macrophages was significantly increased in CSF of patients compared to controls (Fig. S9). We also collected peripheral blood samples from patients with thoracic or cervical segment injuries (Table 1) and control donors (Table 3) without SCIs to investigate whether the paracaspase MALT1 was involved in the recovery of SCIs in humans. Peripheral blood monocytes (PBMCs) were isolated from these blood samples and used to detect MALT1, its canonical substrate CYLD, and cleaved product CYLD-Ct. Western blot analyses revealed increased levels of CYLD-Ct in PBMCs from patients with SCIs compared with control samples (Fig. 6

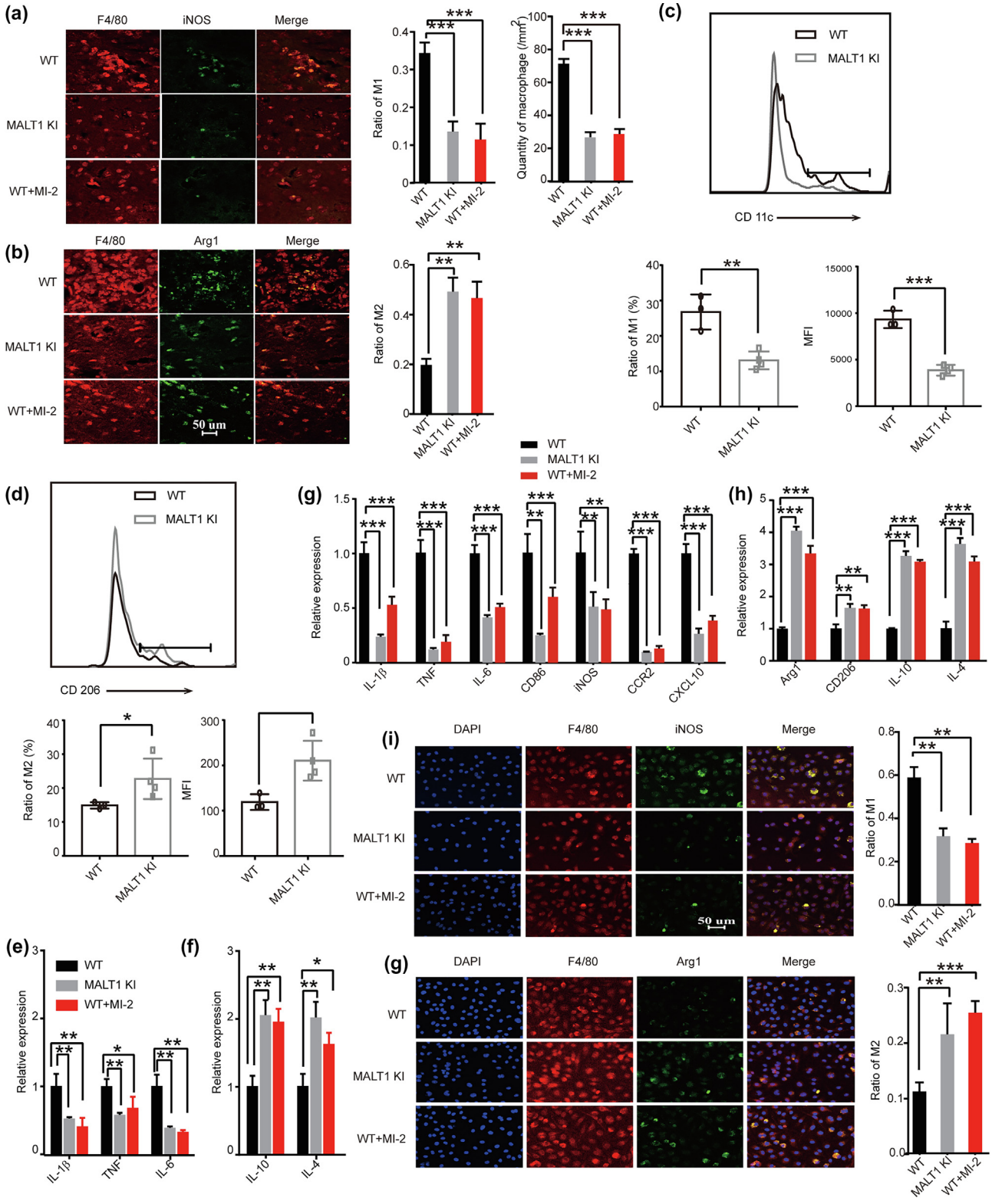

Fig. 4. MALT1 paracaspase activity regulates inflammatory cytokine production and macrophage shift. (a, b) Mice underwent SCI surgery and were treated with MI-2 or PBS as in Fig. 1. The spinal cord was isolated 6 weeks post SCI and stained for F4/80, iNOS or Arg1 for confocal microscopy analyze. Macrophages (F4/80 +) in these slides were quantified and the proportion of pro-inflammatory macrophage (F4/80 + iNOS +) or anti-inflammatory macrophage (F4/80 + Arg1 +) were also assessed (n = 6 mice per group). (c, d) Lymphocytes infiltrating the spinal cord were isolated 3 days post SCI and stained for F4/80, CD11c (pro-inflammatory macrophage) or CD206 (anti-inflammatory macrophage), and then analyzed by FACS. Representative stainings, quantitative analysis of pro-inflammatory macrophage or anti-inflammatory macrophage percentages and mean fluorescence intensities (MFI) were shown. (n = 3 for WT and n = 4 for MALT1 KI group). (e, f) The spinal cord tissues were isolated from the injury sites 3 days post SCI and used for realtime PCR analysis of pro-inflammatory factors and anti-inflammatory factors (n = 6 mice for each group). (G&J) BMDMs were generated from WT or MALT-1 KI mice and incubated with MI-2 (4 μmol/L) or PBS for 4 h. Cells were then treated with LPS (100 ng/mL) plus IFN-γ (10 ng/mL) for pro-inflammatory macrophage or with IL-4 (10 ng/mL) for anti-inflammatory macrophage. After 6 h (pro-inflammatory macrophage) or 24 h (anti-inflammatory macrophage) treatment, the shift of macrophages was detected by RT-PCR (G&H, n = 3 mice per group) or immunofluorescent staining (i,j, n = 6 mice per group). $^{*}P < 0.05$, $^{**}P < 0.01$, $^{***}P < 0.001$.

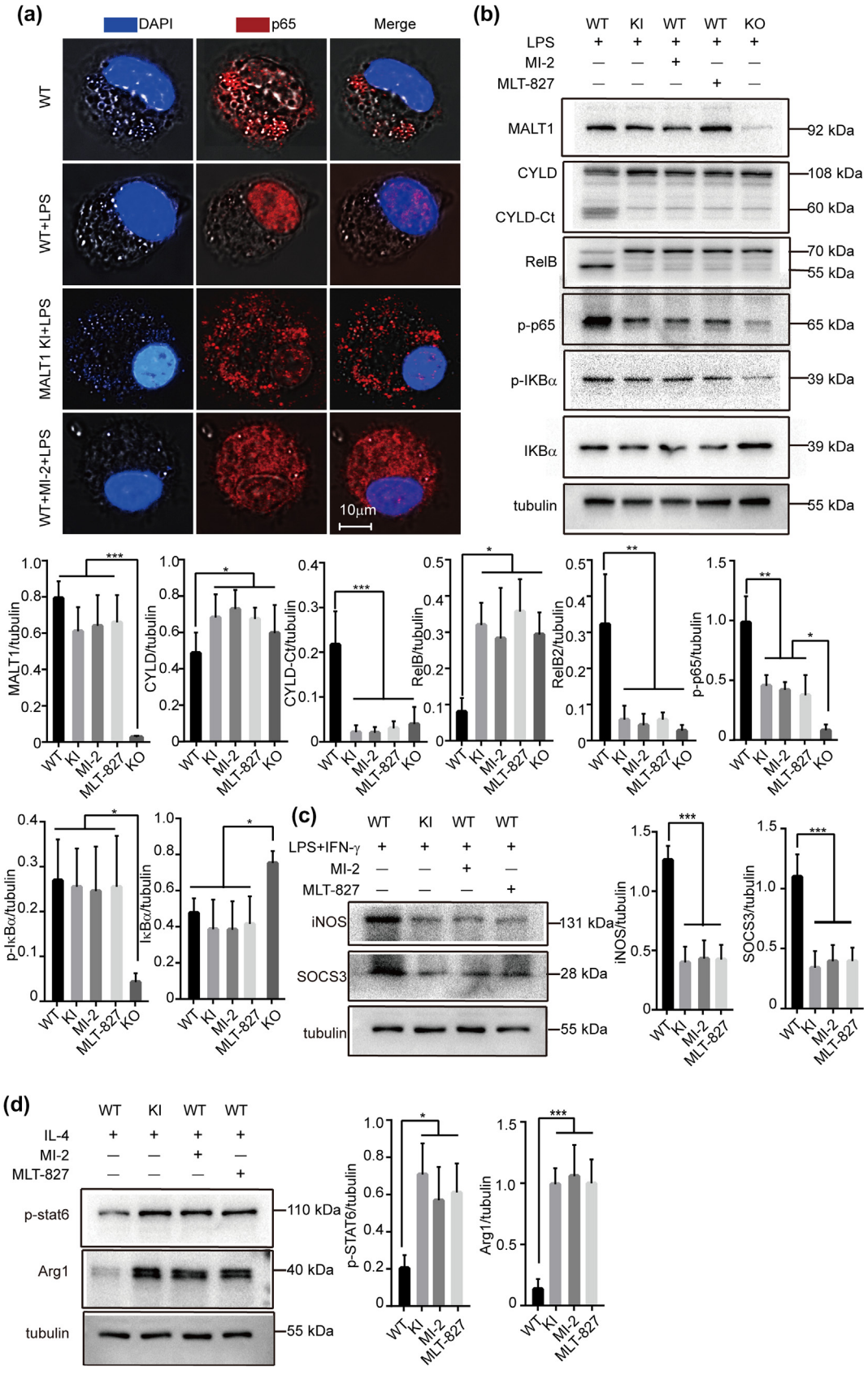

Fig. 5. Deficiency in MALT1 paracaspase activity decreases NF-κB activation and reduces SOCS3 levels. (a) WT BMDMs, MI-2-pretreated (4 μmol/L for 4 h) BMDMs and MALT1 KI BMDMs were treated with LPS for 30 min. The localization of p65 was examined by immunofluorescent staining (scale bar, 10 μm). (b) BMDMs from indicated mice were pretreated with either MI-2 (4 μmol/L for 4 h), MLT-827 (3 μmol/L for 1 h) or PBS and then stimulated with LPS (100 ng/mL) for 30 min. Protein extracts were used for Western blot analysis. (BMDMs were pretreated as in (b) and stimulated with LPS (100 ng/mL) plus IFN-γ (10 ng/mL) for 6 h (c) or with IL-4 (10 ng/mL) for 24 h (d). The protein extracts were used for Western blot analysis. $^{*}P < 0.05$, $^{**}P < 0.01$, $^{***}P < 0.001$. Data are representative of at least three independent experiments.

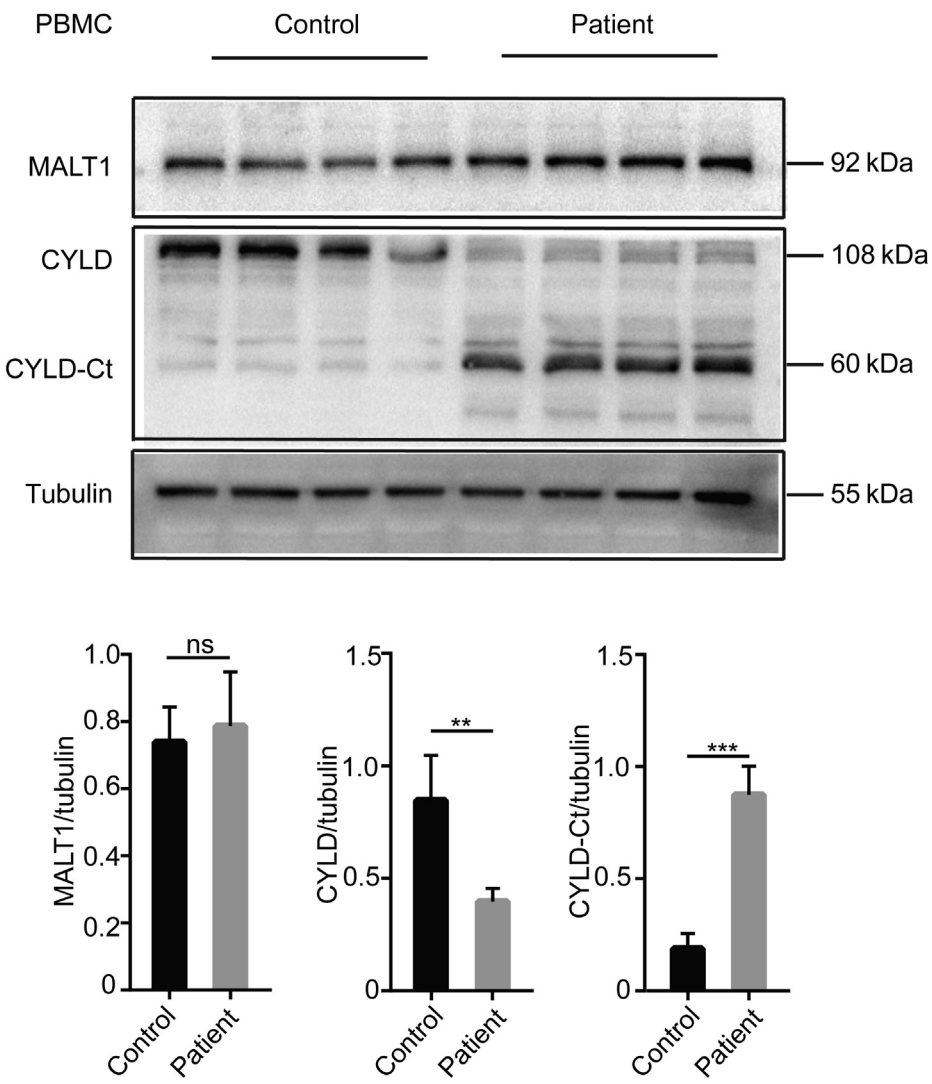

Fig. 6. High MALT1 activity is detected in patients with SCI. PBMCs were collected from SCI patients 48 h post injury and from healthy subjects. The expression level and paracaspase activity of MALT1 (cleavage of CYLD to CYLD-Ct) in the PBMCs were examined by Western blot. Each line represents an independent biological sample. Data are representative of two independent experiments. $^{*}P < 0.05$, $^{**}P < 0.01$, $^{***}P < 0.001$.

and Fig. S7). Thus, the paracaspase activity of MALT1 was up-regulated in patients after SCIs.

3.7. MALT1 paracaspase activity and NF-κB signaling pathway are required for a shift of human monocyte-derived macrophages (hMDMs)

To investigate whether MALT1 paracaspase activity is also involved in monocyte-derived macrophage (MDM) shift, peripheral blood samples from healthy donors were collected to isolate monocytes and cultured to differentiate them into hMDMs in vitro. Half of the cells were treated with MI-2 (4 μmol/L for 4 h) or MLT-827 (3 μmol/L for 1 h) and then stimulated with LPS. Human MDMs showed high levels of MALT1 paracaspase activity upon activation with LPS, which was significantly blocked by the small molecules MI-2 and MLT-827 (Fig. 7a). Phosphorylation of p-65 also lessened after inhibition of MALT1 paracaspase activity (Fig. 7a). In addition, the expression of the pro-inflammatory macrophage marker, iNOS, decreased (Fig. 7b), and the level of the anti-inflammatory macrophage marker, Arg1, increased when MALT1 paracaspase was inhibited (Fig. 7c). Thus, hMDMs and mBMDM may both use a similar signaling axis, relying on the MALT1 paracaspase and NF-κB to determine their shift, suggesting that inhibition of MALT1 paracaspase activity could be a potential approach to improve functional recovery after SCI.

4. Discussion

SCI is devastating for afflicted individuals, frequently resulting in permanent impairments due to limited prospects for normal regeneration. Destruction of the blood-spinal cord barrier in patients with SCI elicits rapid lymphocyte infiltration and massive inflammation, which leads to further tissue damage. Lymphocytic infiltration and inflammation are also hallmarks of EAE and it was shown that MALT1 paracaspase deficiency reduces the inflammatory reactions in the CNS of mice with EAE [33,34,59], Thus, we hypothesized that blocking MALT1 paracaspase function, might promote functional recovery after SCI. Our current research verified this hypothesis and revealed a previously unknown consequence of MALT1 paracaspase deficiency/inhibition in ameliorating SCI.

In this study, we discovered that the paracaspase activity of MALT1 was increased in peripheral blood samples from patients with SCI (Fig. 6, Fig. S7 online). We introduced a targeted mutation

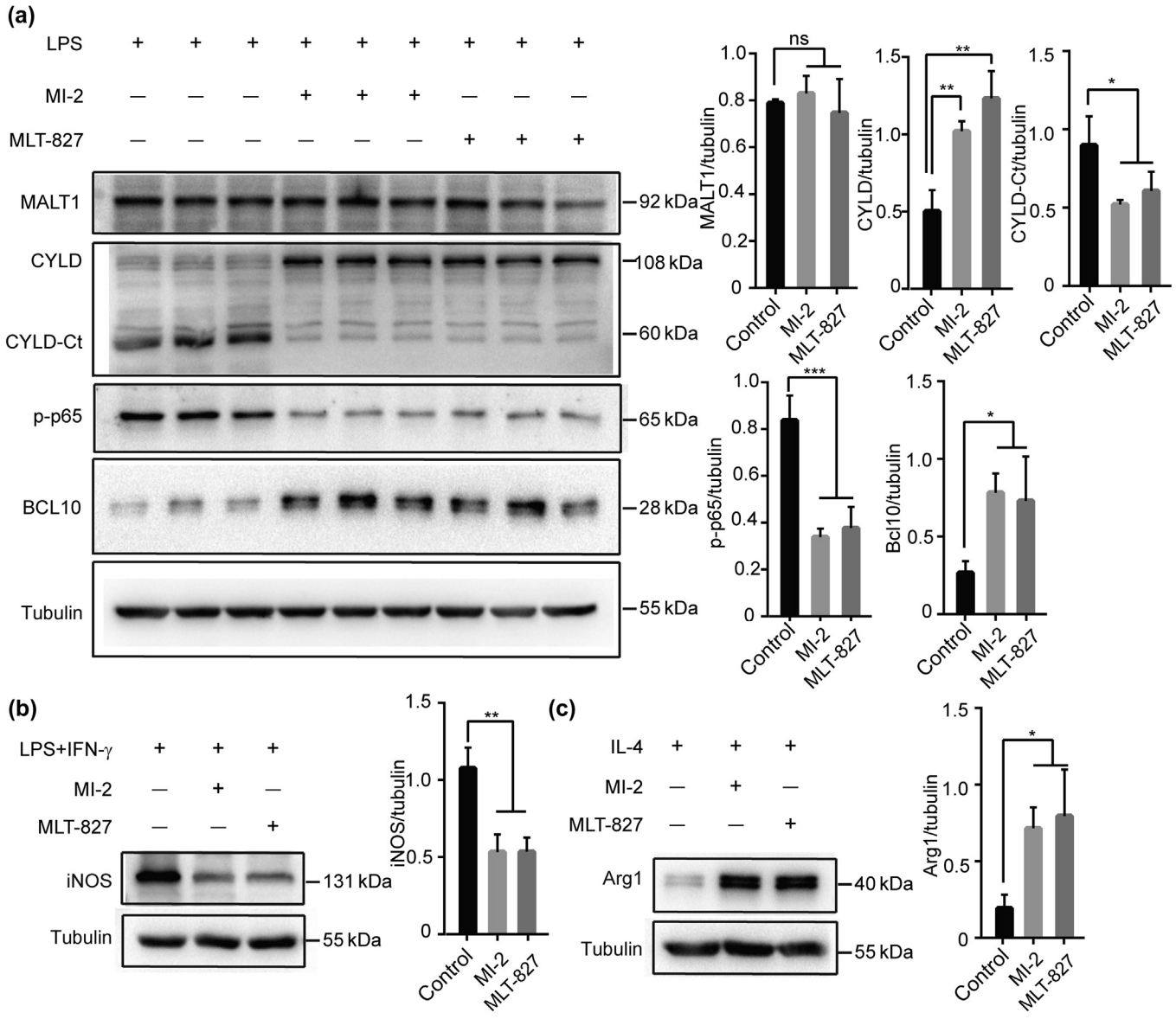

Fig. 7. MALT1 paracaspase activity regulates hMDMs shift *in vitro*. (a) hMDMs were isolated from the blood of healthy human subjects, pretreated with MI-2 (4 μmol/L for 4 h) or MLT-827 (3 μmol/L for 1 h) and then stimulated with LPS (100 ng/mL) for 30 min. Protein extracts were used for Western blot analysis. Data represent samples from three human subjects. hMDMs were pre-incubated with MI-2 or MLT-827 as in A and then treated with LPS (100 ng/mL) plus IFN-γ (20 ng/mL) for 6 h (b) or with IL-4 20 ng/mL) for 18 h (c). The shift of hMDMs was determined by Western blot. Data are representative of three independent experiments. $^{*}P < 0.05$, $^{**}P < 0.01$, $^{***}P < 0.001$.

in the caspase-like domain of the MALT1 in mice (MALT1 KI mice) and used the previously described SCI model to determine the effects of MALT1 paracaspase activity on SCI. The mutation significantly reduced the paracaspase activity of MALT1 without affecting the levels of its protein, confirming previous reports [34,38,56] (Fig. S1e online). An important observation from our study was that the genetic mutation of MALT1 resulted in improved neurological recovery following SCI (Fig. 1). Pharmacological inhibition of the paracaspase activity of MALT1 by MI-2 also improved recovery following SCI (Fig. 1). Thus, a deficiency in MALT1 paracaspase activity protected mice from SCI.

One of the striking findings from our study was the discovery that MALT1 paracaspase activity in macrophages is essential for functional recovery after SCI. Using bone marrow chimeras, as well as adoptively transfer macrophages, we demonstrated that manipulation of MALT1 paracaspase activity in macrophages was a critical component of functional recovery upon SCI (Figs. 2, 3). Furthermore, we determined that MALT1 paracaspase activity in macrophages affected their ability for migration and differentiation (Fig. 4, Fig. S6 online). Indeed, macrophages from KI mice as well as those treated with the MALT1 inhibitors (MI-2), showed reduced levels of CCR2 and CXCR10, and significantly lower amounts of macrophages being recruited into the injury site (Fig. 4g). According to Popovich et al, decreased macrophage accumulation at the SCI site exerts a neuroprotective effect and facilitates loco-motor recovery [60]. It has been reported that levels of CCR2 and CXCL10 are key contributors to macrophage migration in SCI [50,52,61]. Thus, the deficiency in MALT1 paracaspase activity might decrease macrophage infiltration in the mouse SCI model by down-regulating CCR2 and CXCL10.

It has been well documented that macrophages can be polarized into two distinct phenotypes following SCI [13,18,19,22,62,63]. A depletion of pro-inflammatory macrophage phenotypes improves recovery [60], while an increase in reparative macrophage phenotypes increases axon growth and motor function [64]. In particular, pro-inflammatory macrophages are

recruited during the acute response to trauma and release high levels of pro-inflammatory cytokines, such as TNF, IL-6, and IL-1β, while anti-inflammatory macrophages produce high levels of anti-inflammatory cytokines, such as IL-10 and IL-4, and exhibit tissue repair properties [65,66]. These cytokines are important components of posttraumatic inflammation and play critical roles in regulating functional recovery [67,68]. Our recent study demonstrated that blocking IFN-γ-mediated macrophage activation and inflammatory cytokine production significantly improved functional recovery upon SCI [12]. Our research also demonstrated that suppression of the MALT1 paracaspase activity, either genetically with KI mice, or with small molecule inhibitors, pushed the macrophages towards an anti-inflammatory phenotype, and reduced the number of pro-inflammatory macrophages, both *in vitro* and in vivo (Fig. 4). Therefore, the deficiency in MALT1 paracaspase activity protected mice from SCI by promoting macrophage shift towards a reparative phenotype, while decreasing shift towards a pro-inflammatory phenotype. Further studies are required to determine whether the altered MALT1 paracaspase activity can also regulate the functions of other cell subsets that participate in the inflammatory reactions in SCI.

Previous reports have demonstrated that MALT1 functions in two ways: MALT1-scaffold dependent IkB phosphorylation-degradation and MALT1-paracaspase activity dependent cleavage of substrates [36,69]. Other groups showed that C472Gmutation or MI2/MLT-827 inhibition significantly reduced the paracaspase activity of MALT1, but maintained its scaffold function [34,38,56]. We also determined that the scaffold function of MALT1 was largely unaffected when its protease function was blocked, as indicated by IκB phosphorylation and degradation (Fig. 5b). What is the underlining molecular mechanism used by the MALT1 paracaspase to regulate macrophage differentiation?

The role of MALT1 in mediating LPS cellular effects has remained controversial for several years. In 2003, the pioneering two studies reporting on the generation of MALT1 KO mice corroborated together, with the exception of LPS-driven splenocyte proliferation, which was fully dependent on MALT1 in one study [70] and completely independent of MALT1 in the other study [24]. Since then, other reports were published; however, the conundrum has not yet been resolved. In 2006, Dong et al., using the murine macrophage cell line RAW 264.7, reported that MALT1 is required downstream of TLR-4, to mediate BCL10- and TRAF6-dependent NF-κB activation [71]. Using caspase recruitment domain (CARD)-9 deficient bone marrow derived dendritic cells, Hara et al. reported that CARD9 is required for cytokine production (e.g. TNF) downstream of TLR-4 [72]. However, more data has shown that CARD9-dependent MALT1 proteolytic activity is required for TNF production in myeloid cells via dectin-1 pathway, downstream of C-type lectin-like selected receptors [37,73]. In B lymphocytes, there is evidence for crosstalk between the B-cell

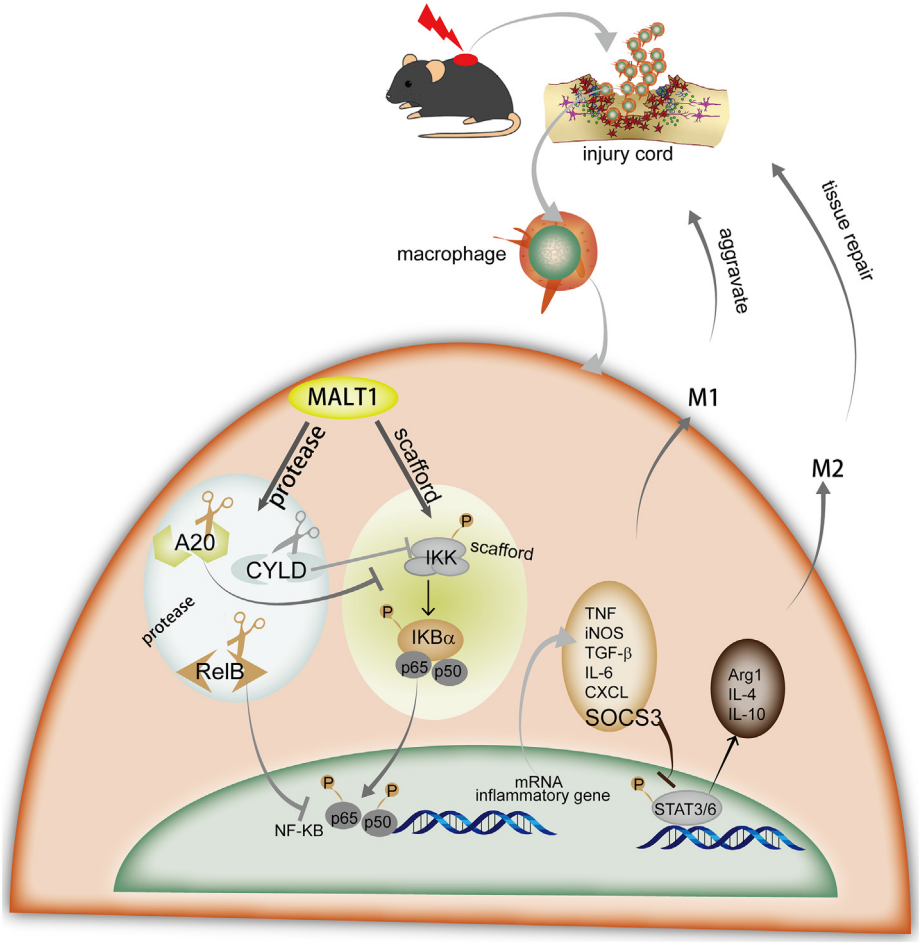

Fig. 8. (Color online) Diagram of MALT1 action in spinal cord injury. Upon SCI injury and stimulation by cell debris, MALT1 in macrophages initiates the degradation of A20, CYLD and RelB and activation of NF-κB signaling. Activated NF-κB triggers the production of many inflammatory factors as well as socs3, which suppresses the activation of STAT6 and anti-inflammatory macrophage shift. Inflammatory macrophages aggravate inflammation in the trauma lesions and induce secondary damage. Deficiency in/inhibition of MALT1 paracaspase activity reduce the activation of NF-κB signaling and promotes the generation of anti-inflammatory macrophages, which promotes recovery from SCI.

receptor and the TLR-4 receptor pathways [74]. The TLR-4 pathway might also be able to crosstalk with alternative pathways in myeloid cells. In this regard, recent evidence indicates that TRAF6 can regulate MALT1 paracaspase activity and might be able to activate MALT1 independent of CARD/BCL10 [75,76]. In fact, there might be alternative routes leading to MALT1 activation other than the canonical CBM pathway, although this is just starting to be explored [30]. Moreover, two isoforms of MALT1 were recently described, whose expression and regulatory function are still not well understood [77]. Therefore, one may hypothesize that, under certain circumstances and using a mechanism that remains to be defined, the recruitment of MALT1 (likely its isoform A) to TRAF6 may serve as a point of crosstalk for regulation of the TLR-4 pathway. Finally, intracellular LPS signaling was also described [78] and it cannot be excluded that this pathway might contribute to MALT1 activation, as this hypothesis has not been tested yet.

We found that LPS stimulation drives the translocation of p65 from cytosol to nucleus in macrophages. Deficiency or inhibition of MALT1 paracaspase activity blocks the translocation of p65 in response to LPS stimulation (Fig. 5a). Thus MALT1 promotes the activation and translocation of NF-κB upon LPS stimulation. The NF-κB pathway has a central role in pro-inflammatory macrophage shift by controlling inflammation via production of pro-inflammatory cytokines [55,79–81]. As expected, we observed significantly reduced NF-κB activation in MALT1 paracaspase activity-deficient macrophages in SCI (Fig. 5, b). Moreover, SOCS family members, which inhibit the phosphorylation of STAT6, biased macrophages to differentiate into the pro-inflammatory macrophages [57,58]. Also, SOCS3 was expressed at lower levels and STAT6 phosphorylation was increased in MALT1 paracaspase activity-deficient macrophages when compared with control macrophages, under anti-inflammatory differentiation conditions (Fig. 5c, d). In general, the deficiency in MALT1 paracaspase activity predisposed macrophages to differentiate into the anti-inflammatory macrophages by attenuating the activity of NF-κB – SOCS signaling pathways. More importantly, blood samples from patients with SCI showed higher MALT1 paracaspase activity (Fig. 6 and Fig. S7 online), and responded to MALT1 protease inhibition with reduced pro-inflammatory macrophage shift and enhanced anti-inflammatory macrophage shift (Fig. 7). Thus, it is the protease function of MALT1 that is significant for macrophage differentiation as investigated here.

Collectively, our results strongly support the hypothesis that the inhibition of MALT1 paracaspase activity attenuates NF-κB and SOCS3 signaling in macrophages, subsequently reducing inflammation and biased anti-inflammatory response and thus promoting tissue repair after SCI (Fig. 8). Therefore, our study revealed a protective effect of MALT1 inhibition on improving SCI recovery and might provide a novel therapeutic target for SCI treatments. This suggests potential avenues for using MALT1 inhibitors in acute clinical settings and avoiding safety issues that might arise upon chronic MALT1 inhibition [82].

Conflict of interest

The authors declare that they have no conflict of interests.

Acknowledgments

This work was supported by the National Natural Science Foundation of China (31470872 to YG and 31400770 to ZY), the "111" project (B16021 to YG and ZY), the Science and Technology Program of Guangzhou (201604020162 to YG), Science & Technology Planning and Key Technology Innovation Projects of Guangdong (201803010001 to ZL), the National Natural Science Foundation of Guangdong (2018A030313576 to GS), Traditional Chinese Medicine Bureau of Guangdong (20181071 to JH), the National Natural Science Foundation of China (31800721 to QW), Medical and Health Development Plan of Shandong Province (2017WS446 to LZ). We wish to thank Hezuo Lü for providing technical support with the animal models.

Author contributions

H. Zhang and G. Sun developed the hypothesis, designed experiments, performed the experiments, and contributed to editing the manuscript. X. Li and Z. Fu contributed to cutting tissues into slices. G. Cao and Q. Wang helped in English language editing of this manuscript. S. Yang, J. Zhu, D. Li, L. Zheng, X. Xia, P. Li, J. Li and W. Zhou provided administrative, technical, and material support. J. Hao and L. Zhang provided detection of ELISA. Z. Li and L. Zhou provided the experimental instrument. F. Bornancin contributed MLT-827 and provided comments. Y. Gao and Z. Yin supervised the study and helped the manuscript editing and discussions.

Appendix A. Supplementary data

Supplementary data to this article can be found online at https://doi.org/10.1016/j.scib.2019.04.026.

References

[1] Okada S, Nakamura M, Katoh H, et al. Conditional ablation of stat3 or socs3 discloses a dual role for reactive astrocytes after spinal cord injury. Nat Med 2006;12:829–34.
[2] Allan SM, Tyrrell PJ, Rothwell NJ. Interleukin-1 and neuronal injury. Nat Rev Immunol 2005;5:629–40.
[3] Beattie MS. Inflammation and apoptosis: linked therapeutic targets in spinal cord injury. Trends Mol Med 2004;10:580–3.
[4] Ruff CA, Wilcox JT, Fehlings MG. Cell-based transplantation strategies to promote plasticity following spinal cord injury. Exp Neurol 2012;235:78–90.
[5] Ambrozaitis KV, Kontautas E, Spakauskas B, et al. pathophysiology of acute spinal cord injury. Medicina 2006;42:255–61.
[6] Dumont RJ, Okonkwo DO, Verma S, et al. Acute spinal cord injury, part i: pathophysiologic mechanisms. Clin Neuropharmacol 2001;24:254–64.
[7] Dumont RJ, Verma S, Okonkwo DO, et al. Acute spinal cord injury, part ii: contemporary pharmacotherapy. Clin Neuropharmacol 2001;24:265–79.
[8] Hayashi K, Hashimoto M, Koda M, et al. Increase of sensitivity to mechanical stimulus after transplantation of murine induced pluripotent stem cell-derived astrocytes in a rat spinal cord injury model. J Neurosurg Spine 2011;15:582–93.
[9] Fehlings MG, Cadotte DW, Fehlings LN. A series of systematic reviews on the treatment of acute spinal cord injury: a foundation for best medical practice. J Neurotrauma 2011;28:1329–33.
[10] Pineau I, Lacroix S. Proinflammatory cytokine synthesis in the injured mouse spinal cord: multiphasic expression pattern and identification of the cell types involved. J Comp Neurol 2007;500:267–85.
[11] Popovich PG. Neuroimmunology of traumatic spinal cord injury: a brief history and overview. Exp Neurol 2014;258:1–4.
[12] Sun G, Yang S, Cao G, et al. Γδ t cells provide the early source of ifn-γ to aggravate lesions in spinal cord injury. J Exp Med 2018;215:521–35.
[13] David S, Kroner A. Repertoire of microglial and macrophage responses after spinal cord injury. Nat Rev Neurosci 2011;12:388–99.
[14] Donnelly DJ, Popovich PG. Inflammation and its role in neuroprotection, axonal regeneration and functional recovery after spinal cord injury. Exp Neurol 2008;209:378–88.
[15] Yong VW, Rivest S. Taking advantage of the systemic immune system to cure brain diseases. Neuron 2009;64:55–60.
[16] Biswas SK, Chittezhath M, Shalova IN, et al. Macrophage polarization and plasticity in health and disease. Immunol Res 2012;53:11–24.
[17] Mantovani A, Vecchi A, Allavena P. Pharmacological modulation of monocytes and macrophages. Curr Opin Pharmacol 2014;17:38–44.
[18] Kigerl KA, Gensel JC, Ankeny DP, et al. Identification of two distinct macrophage subsets with divergent effects causing either neurotoxicity or regeneration in the injured mouse spinal cord. J Neurosci: The Off J Soc Neurosci 2009;29:13435–44.
[19] Shechter R, Schwartz M. Harnessing monocyte-derived macrophages to control central nervous system pathologies: no longer 'if' but 'how'. J Pathol 2013;229:332–46.
[20] Shechter R, London A, Varol C, et al. Infiltrating blood-derived macrophages are vital cells playing an anti-inflammatory role in recovery from spinal cord injury in mice. PLoS Med 2009;6:e1000113.

[21] Mosser DM, Edwards JP. Exploring the full spectrum of macrophage activation. Nat Rev Immunol 2008;8:958–69.
[22] Ren Y, Young W. Managing inflammation after spinal cord injury through manipulation of macrophage function. Neural plasticity 2013;2013:945034.
[23] Shechter R, Miller O, Yovel G, et al. Recruitment of beneficial m2 macrophages to injured spinal cord is orchestrated by remote brain choroid plexus. Immunity 2013;38:555–69.
[24] Ruland J, Duncan GS, Wakeham A, et al. Differential requirement for malt1 in t and b cell antigen receptor signaling. Immunity 2003;19:749–58.
[25] Thome M. Multifunctional roles for malt1 in t-cell activation. Nat Rev Immunol 2008;8:495–500.
[26] Hachmann J, Salvesen GS. The paracaspase malt1. Biochimie 2016;122:324–38.
[27] Sun L, Deng L, Ea CK, et al. The traf6 ubiquitin ligase and tak1 kinase mediate ikk activation by bcl10 and malt1 in t lymphocytes. Mol Cell 2004;14:289–301.
[28] Hailfinger S, Nogai H, Pelzer C, Malt1-dependent,, et al. relb cleavage promotes canonical nf-kappab activation in lymphocytes and lymphoma cell lines. PNAS 2011;108:14596–601.
[29] Staal J, Driege Y, Bekaert T, et al. T-cell receptor-induced jnk activation requires proteolytic inactivation of cyld by malt1. The EMBO J 2011;30:1742–52.
[30] Israel L, Bornancin F. Ways and waves of malt1 paracaspase activation. Cell Mol Immunol 2018;15:8–11.
[31] Mao R, Yang R, Chen X, et al. Regnase-1, a rapid response ribonuclease regulating inflammation and stress responses. Cell Mol Immunol 2017;14:412–22.
[32] Vucic D, Dixit VM. Masking malt1: the paracaspase's potential for cancer therapy. J Exp Med 2009;206:2309–12.
[33] Mc Guire C, Elton L, Wieghofer P, et al. Pharmacological inhibition of malt1 protease activity protects mice in a mouse model of multiple sclerosis. J Neuroinflammation 2014;11:124.
[34] Bornancin F, Renner F, Touil R, et al. Deficiency of malt1 paracaspase activity results in unbalanced regulatory and effector t and b cell responses leading to multiorgan inflammation. J Immunol 2015;194:3723–34.
[35] Fontan L, Yang C, Kabaleeswaran V, et al. Malt1 small molecule inhibitors specifically suppress abc-dlbcl in vitro and in vivo. Cancer Cell 2012;22:812–24.
[36] Bardet M, Unterreiner A, Malinverni C, et al. The t-cell fingerprint of malt1 paracaspase revealed by selective inhibition. Immunol Cell Biol 2018;96:81–99.
[37] Unterreiner A, Stoehr N, Huppertz C, et al. Selective malt1 paracaspase inhibition does not block tnf-alpha production downstream of tlr4 in myeloid cells. Immunol Lett 2017;192:48–51.
[38] Jaworski M, Marsland BJ, Gehrig J, et al. Malt1 protease inactivation efficiently dampens immune responses but causes spontaneous autoimmunity. The EMBO J 2014;33:2765–81.
[39] Meininger I, Krappmann D. Lymphocyte signaling and activation by the carma1-bcl10-malt1 signalosome. Biol Chem 2016;397:1315–33.
[40] Unterreiner A, Touil R, Anastasi D, et al. Myeloid innate signaling pathway regulation by malt1 paracaspase activity. J Visualized Exp: JoVE 2019.
[41] Cheng P, Wang T, Li W, et al. Baicalin alleviates lipopolysaccharide-induced liver inflammation in chicken by suppressing tlr4-mediated nf-kappab pathway. Front Pharmacol 2017;8:547.
[42] Basso DM, Fisher LC, Anderson AJ, et al. Basso mouse scale for locomotion detects differences in recovery after spinal cord injury in five common mouse strains. J Neurotrauma 2006;23:635–59.
[43] Gao Y, Tao J, Li MO, et al. Jnk1 is essential for cd8+ t cell-mediated tumor immune surveillance. J Immunol 2005;175:5783–9.
[44] Koopmans GC, Deumens R, Honig WM, et al. The assessment of locomotor function in spinal cord injured rats: the importance of objective analysis of coordination. J Neurotrauma 2005;22:214–25.
[45] Hamers FP, Lankhorst AJ, van Laar TJ, et al. Automated quantitative gait analysis during overground locomotion in the rat: its application to spinal cord contusion and transection injuries. J Neurotrauma 2001;18:187–201.
[46] Hendriks WT, Eggers R, Ruitenberg MJ, et al. Profound differences in spontaneous long-term functional recovery after defined spinal tract lesions in the rat. J Neurotrauma 2006;23:18–35.
[47] Klapka N, Hermanns S, Straten G, et al. Suppression of fibrous scarring in spinal cord injury of rat promotes long-distance regeneration of corticospinal tract axons, rescue of primary motoneurons in somatosensory cortex and significant functional recovery. Eur J Neurosci 2005;22:3047–58.
[48] Sun GD, Chen Y, Zhou ZG, et al. A progressive compression model of thoracic spinal cord injury in mice: function assessment and pathological changes in spinal cord. Neural Regen Res 2017;12:1365–74.
[49] Hsieh CL, Niemi EC, Wang SH, et al. Ccr2 deficiency impairs macrophage infiltration and improves cognitive function after traumatic brain injury. J Neurotrauma 2014;31:1677–88.
[50] Ka SO, Song MY, Bae EJ, et al. Myeloid sirt1 regulates macrophage infiltration and insulin sensitivity in mice fed a high-fat diet. J Endocrinol 2015;224:109–18.
[51] Morganti JM, Jopson TD, Liu S, et al. Ccr2 antagonism alters brain macrophage polarization and ameliorates cognitive dysfunction induced by traumatic brain injury. J Neurosci: The Off J Soc Neurosci 2015;35:748–60.
[52] Vogel DY, Heijnen PD, Breur M, et al. Macrophages migrate in an activation-dependent manner to chemokines involved in neuroinflammation. J Neuroinflammation 2014;11:23.
[53] Nagel D, Spranger S, Vincendeau M, et al. Pharmacologic inhibition of malt1 protease by phenothiazines as a therapeutic approach for the treatment of aggressive abc-dlbcl. Cancer Cell 2012;22:825–37.
[54] Mann M, Mehta A, Zhao JL, et al. An nf-kappab-microrna regulatory network tunes macrophage inflammatory responses. Nat Commun 2017;8:851.
[55] Pagliari LJ, Perlman H, Liu H, et al. Macrophages require constitutive nf-kappab activation to maintain a1 expression and mitochondrial homeostasis. Mol Cell Biol 2000;20:8855–65.
[56] Gewies A, Gorka O, Bergmann H, et al. Uncoupling malt1 threshold function from paracaspase activity results in destructive autoimmune inflammation. Cell reports 2014;9:1292–305.
[57] Whyte CS, Bishop ET, Ruckerl D, et al. Suppressor of cytokine signaling (socs)1 is a key determinant of differential macrophage activation and function. J Leukoc Biol 2011;90:845–54.
[58] Liu Y, Stewart KN, Bishop E, et al. Unique expression of suppressor of cytokine signaling 3 is essential for classical macrophage activation in rodents in vitro and in vivo. J Immunol 2008;180:6270–8.
[59] Brustle A, Brenner D, Knobbe CB, et al. The nf-kappab regulator malt1 determines the encephalitogenic potential of th17 cells. J Clin Investig 2012;122:4698–709.
[60] Popovich PG, Guan Z, Wei P, et al. Depletion of hematogenous macrophages promotes partial hindlimb recovery and neuroanatomical repair after experimental spinal cord injury. Exp Neurol 1999;158:351–65.
[61] Luster AD, Leder P. Ip-10, a -c-x-c- chemokine, elicits a potent thymus-dependent antitumor response in vivo. J Exp Med 1993;178:1057–65.
[62] Shin T, Ahn M, Moon C, et al. Alternatively activated macrophages in spinal cord injury and remission: another mechanism for repair? Mol Neurobiol 2013;47:1011–9.
[63] Thawer SG, Mawhinney L, Chadwick K, et al. Temporal changes in monocyte and macrophage subsets and microglial macrophages following spinal cord injury in the lys-egfp-ki mouse model. J Neuroimmunol 2013;261:7–20.
[64] Schwartz M, Yoles E. Immune-based therapy for spinal cord repair: autologous macrophages and beyond. J Neurotrauma 2006;23:360–70.
[65] Sindrilaru A, Scharffetter-Kochanek K. Disclosure of the culprits: macrophages-versatile regulators of wound healing. Adv Wound Care (New Rochelle) 2013;2:357–68.
[66] Lucas T, Waisman A, Ranjan R, et al. Differential roles of macrophages in diverse phases of skin repair. J Immunol 2010;184:3964–77.
[67] Satzer D, Miller C, Maxon J, et al. T cell deficiency in spinal cord injury: altered locomotor recovery and whole-genome transcriptional analysis. BMC Neurosci 2015;16:74.
[68] Guizar-Sahagun G, Velasco-Hernandez L, Martinez-Cruz A, et al. Systemic microcirculation after complete high and low thoracic spinal cord section in rats. J Neurotrauma 2004;21:1614–23.
[69] Ruland J, Hartjes L. Card-bcl-10-malt1 signalling in protective and pathological immunity. Nat Rev Immunol 2018.
[70] Ruefli-Brasse AA, French DM, Dixit VM. Regulation of nf-kappab-dependent lymphocyte activation and development by paracaspase. Science 2003;302:1581–4.
[71] Dong W, Liu Y, Peng J, et al. The irak-1-bcl10-malt1-traf6-tak1 cascade mediates signaling to nf-kappab from toll-like receptor 4. J Biol Chem 2006;281:26029–40.
[72] Hara H, Ishihara C, Takeuchi A, et al. The adaptor protein card9 is essential for the activation of myeloid cells through itam-associated and toll-like receptors. Nat Immunol 2007;8:619–29.
[73] Gringhuis SI, Wevers BA, Kaptein TM, et al. Selective c-rel activation via malt1 controls anti-fungal t(h)-17 immunity by dectin-1 and dectin-2. PLoS Pathog 2011;7:e1001259.
[74] Dufner A, Schamel WW. B cell antigen receptor-induced activation of an irak4-dependent signaling pathway revealed by a malt1-irak4 double knockout mouse model. Cell Commun Signal 2011;9:6.
[75] Ginster S, Bardet M, Unterreiner A, et al. Two antagonistic malt1 auto-cleavage mechanisms reveal a role for traf6 to unleash malt1 activation. PLoS ONE 2017;12:e0169026.
[76] Bardet M, Seeholzer T, Unterreiner A, et al. Malt1 activation by traf6 needs neither bcl10 nor card11. Biochem Biophys Res Commun 2018;506:48–52.
[77] Meininger I, Griesbach RA, Hu D, et al. Alternative splicing of malt1 controls signalling and activation of cd4(+) t cells. Nat Commun 2016;7:11292.
[78] Yi YS. Caspase-11 non-canonical inflammasome: a critical sensor of intracellular lipopolysaccharide in macrophage-mediated inflammatory responses. Immunology 2017;152:207–17.
[79] Beg AA, Finco TS, Nantermet PV, et al. Tumor necrosis factor and interleukin-1 lead to phosphorylation and loss of i kappa b alpha: a mechanism for nf-kappa b activation. Mol Cell Biol 1993;13:3301–10.
[80] Libermann TA, Baltimore D. Activation of interleukin-6 gene expression through the nf-kappa b transcription factor. Mol Cell Biol 1990;10:2327–34.
[81] Luan H, Zhang Q, Wang L, et al. Om85-bv induced the productions of il-1β, il-6, and tnf-α via tlr4-and tlr2-mediated erk1/2/nf-κb pathway in raw264. 7 cells. J Interferon Cytokine Res 2014;34:526–36.
[82] Demeyer A, Staal J, Beyaert R. Targeting malt1 proteolytic activity in immunity, inflammation and disease: good or bad? Trends Mol Med 2016;22:135–50.

Hua Zhang is a Ph.D. candidate at the Biomedical Translational Research Institute, Jinan University Her research interests include Tumor immunity and CNS injury.

Zhinan Yin is a professor and the Dean of the Biomedical Translational Research Institute, Jinan University. He obtained his Ph.D. degree from the Free University of Berlin, Germany. Dr. Yin's research interests include (1) γδ T cell differentiation and regulation; (2) γδ T cell in obesity; (3) γδ T cell function in tumor immunology.

Guodong Sun is an associate chief physician at the Department of Orthopedics, First Affiliated Hospital, Jinan University. He obtained his Ph.D. degree in 2017 from Jinan University. Dr. Sun's research interest focuses on spinal cord injury.

Yunfei Gao is a professor at the Biomedical Translational Research Institute, Jinan University. He obtained his Ph.D. degree from Peking University. Dr. Gao's research interests include (1) tumor immunity; (2) metabolism and immunity; and (3) inflammation and disease.

Zhizhong Li is a professor and the Vice Dean of the Department of Orthopedics, First Affiliated Hospital, Jinan University. He is also the Dean of Department of Orthopedics, Heyuan People's Hospital (Heyuan Affiliated Hospital of Jinan University). Dr. Li obtained his Ph.D. degree from Jinan University. His research interests include surgical treatment of spinal diseases.